Use of CR-39 in Pd/D co-deposition experiments[*]

P.A. Mosier-Boss[1,a], S. Szpak[1], F.E. Gordon[1], and L.P.G. Forsley[2]

[1] SPAWAR Systems Center San Diego, Code 2373, San Diego, CA 92152, USA
[2] JWK International Annandale, VA 22003, USA

Abstract. The use of CR-39, a solid state nuclear track detector, to detect the emission of energetic charged particles during Pd/D co-deposition is demonstrated. The pits observed in the CR-39 are attributed to the Pd/D cathode and are not due to radionuclide contamination in the cell components; nor to the impingement of D_2 bubbles on the surface of the CR-39; nor to chemical attack by D_2, O_2, or Cl_2. The features (i.e., optical contrast, shape, and bright spot in the center of the pit) of the pits generated during Pd/D co-deposition are consistent with those observed for pits that are of a nuclear origin.

1 Introduction

CR-39 is a thermoset resin made by the polymerization of diethyleneglycol bis allylcarbonate in the presence of di-isopropyl peroxydicarbonate catalyst. The resultant cross-linked polymer is chemically resistant and exhibits high abrasion and impact resistance. The most common use of CR-39 is in optics. However, CR-39 has also found use as a solid state nuclear track detector [1]. When traversing a plastic material such as CR-39, charged particles create along their ionization track a region that is more sensitive to chemical etching than the rest of the bulk [2]. After treatment with an etching agent, tracks remain as holes or pits which can be seen with the aid of an optical microscope. The size, depth of penetration, and shape of these tracks provides information about the mass, charge, energy and direction of motion of the particles [3]. For example, if particles enter the surface at normal incidence, the pits are circular. Elliptical tracks result from particles enetring the surface at an angle. The orientation of the elliptical pit mouth indicates the direction of incidence.

As a solid state nuclear track detector, CR-39 has been used for radon monitoring [4], to measure the yields of alpha particles in fusion reactions in plasmas produced by picosecond laser pulses [5], and to characterize the charged particles formed during inertial-confinement fusion experiments [6]. Stacks of CR-39 have been used to detect and characterize cosmic particle reactions on board the International Space Station [7]. CR-39 and other solid state nuclear track detectors have also found use in the

biomedical sciences for monitoring purposes [4,8]. There have been reports of using CR-39 to detect particle emission from Pd/D and Pd/H substrates. CR-39 was used to detect charged particles in gas permeation experiments using Pd foil and D_2 [9]. Recently the use of CR-39 to detect the emission of charged particles during electrolysis in heavy [10,11] and light water [12] has been reported. In the heavy water experiments done by Oriani and Fisher [10], the CR-39 detectors were placed below and above the palladium cathodes (sheets with dimensions of $25 \, mm \times 25 \, mm \times 1 \, mm$). This was the closest the detectors could be placed to the cathode without impeding the uniform loading of the palladium with deuterium. Charged particles cannot travel very far $-4 \, cm$ at most in air, even shorter distances in a liquid such as heavy water. Consequently this experimental configuration is not the most favorable for charged particle detection. Despite this, for 19 electrolysis experiments, charged particle track densities between 150–3760 tracks cm^{-2} were measured (16 control experiments yielded densities between 59–541 tracks cm^{-2}).

Lipson et al. [11,12]. conducted in-situ electrolysis experiments in both heavy and light water using thin Pd metal films. The CR-39 detectors were in direct contact with the Pd metal films. As a result, this experimental configuration is more favorable to detect charged particles emitted from the Pd film during electrolysis. The thickness of the metal films was sufficient to block background sources of charged particles from reaching the CR-39 detectors. Analysis of the CR-39 detectors showed the presence of energetic charged particle tracks (alpha-particles and protons) concentrated in active areas where the cathode was in contact with the CR-39. In these "hot zones" (typically covering areas $0.2 \times 0.5 \, mm^2$ in dimension),

---

[*] Figures S1–S5 are only available in electronic form at http://www.edpsciences.org/epjap.

[a] e-mail: pam.boss@navy.mil
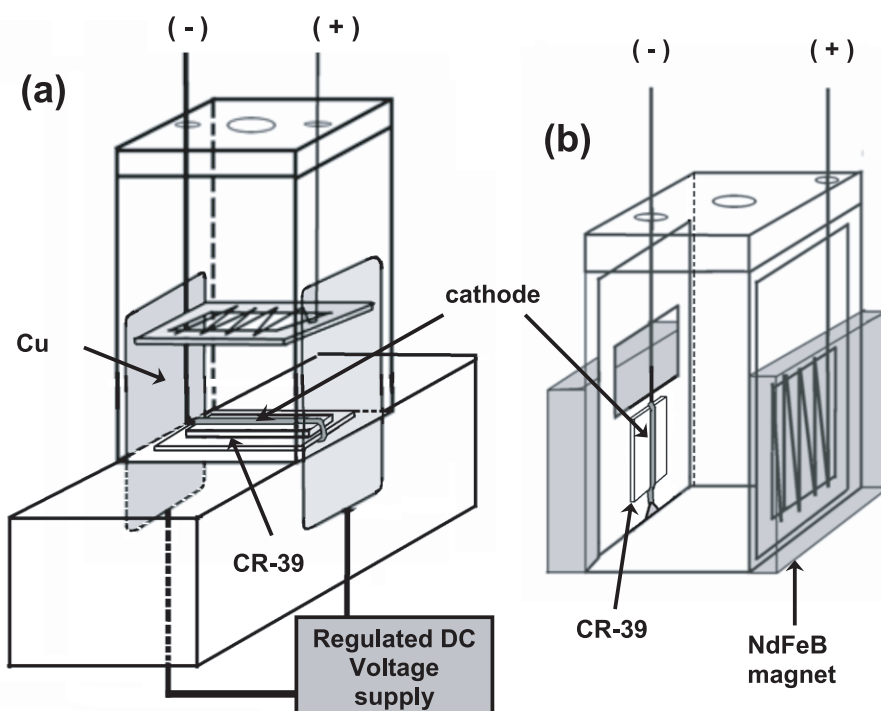
Fig. 1. Schematics of the electrochemical cells used for (a) external electric field experiment and (b) external magnetic field experiment. Single wire cathode configuration is shown. Other cathode configurations include the use of screens and three wires, both parallel and in series.

~200 tracks were detected. Additional experiments were conducted by placing thin Cu and Al foils between the Pd cathode and the CR-39 detector to differentiate between alpha particles and protons and to determine the energies of the charged particles. These experiments showed that 11–16 MeV alpha particles and 1.7 MeV protons were emitted from the Pd cathode during electrolysis.

In this communication, the use of CR-39 to detect charged particles in the Pd/D co-deposition experiment is demonstrated. In these experiments, pits are observed in a CR-39 detector that has been in contact with a cathodically polarized Pd/D substrate. Evidence is presented that show that these pits are tracks caused by the emission of charged particles and that these tracks are not due to either radioactive contamination; or from the electrolysis of heavy water; or from chemical reaction with D_2, O_2, or Cl_2.

2 Experimental

2.1 Materials

Palladium chloride (Aldrich), lithium chloride (Mallinckrodt), deuterated water (Aldrich), HPLC grade light water (Aldrich), sodium hydroxide (Baker), potassium chloride (Aldrich), copper chloride (Aldrich), 0.25 mm diameter gold wire (Aldrich), 0.5 mm diameter silver wire (Aldrich), 0.25 mm diameter platinum wire (Aldrich), 0.25 mm diameter palladium wire (Johnson Matthey), nickel screen (Delker, 0.35 mm thick and eyelet

dimensions of 3 mm × 1.9 mm), 0.025 mm thick gold foil (Aldrich), and copper screen (TWP, Inc., 0.27 mm thick and eyelet dimensions of 1.37 mm × 1.37 mm) were used as received. CR-39 detectors (Fukuvi), rectangular shape with dimensions of 1 cm × 2 cm × 1 mm, were obtained from Landauer and used as received.

2.2 Cell design

Figure 1 shows schematics of the electrochemical cells used to generate the energetic particles. The rectangular cells (Ridout Plastics) were made of butyrate. The anode consisted of platinum wire mounted on a polyethylene base, as shown in Figure 1. In the simplest case, shown in Figure 1, the cathode is comprised of a single wire (Ag or Au). As illustrated in Figure 1, the wire is in contact with a CR-39 detector, which is mounted on a polyethylene base. Other cathode configurations that have been used include a Ni screen or three wires in contact with the CR-39 detector. In the three wire experiments, either different metallic (Ag, Au, and Pt) wires were connected in series or wires of the same type (Ag or Au) were connected in parallel. The latter three wire configuration provides a means to examine the phenomenon as a function of time. CR-39, like photographic film, is a type of detector that is constantly integrating, which means that events are recorded accumulatively. When the wires are connected in parallel, they can be disconnected sequentially at different time intervals. The anode and cathode were connected to a potentiosatat/galvanostat (PAR model 363).

2.3 Charging procedure

Typically 20–25 mL solution of 0.03 M palladium chloride and 0.3 M lithium chloride in deuterated water is added to the cell. Palladium is then plated out onto the cathode substrate using a charging profile of 100 μA for 24 h, followed by 200 μA for 48 h followed by 500 μA until the palladium has been plated out. This charging profile assures good adherence of the palladium on the electrode substrate. Once the palladium has been plated out of solution, the external electric or magnetic fields are applied. In the external electric field configuration, Figure 1a, copper electrodes are taped to the outside of the cell wall. A regulated high voltage source (EMCO model 4330) is used to apply 6000 V DC (and has a ~6% AC component) across these copper electrodes. The external electric field experimental configuration was employed for the no field experiments. In the magnetic field configuration, the attractive forces between the 1 in × 1 in × 0.25 in permanent NdFeB magnets (Dura Magnetics) hold them in place on either side of the cell, as shown in Figure 1b. The strength of the magnetic field is on the order of 2500 Gauss. After the palladium has been electrochemically plated out and the external field has been applied, the cathodic current is increased to 1 mA for 2 h, 2 mA for 6 h, 5 mA for 24 h, 10 mA for 24 h, 25 mA for 24 h, 50 mA for 24 h, 75 mA for 24 h, and 100 mA for 24 h.

## 2.4 Etching of CR-39 and analysis of etched CR-39 detector

When the experiment was terminated, the cell was disassembled and the CR-39 detector was etched in an aqueous 6.5 N sodium hydroxide solution at 65–72 °C for 6–7 h.

Microscopic examination of the etched CR-39 detectors was done using an Eclipse E600 epifluorescent microscope (Nikon) and CoolSnap HQ CCD camera (Photometrics). Magnifications of 20× to 1000× were used.

Scanning of the CR-39 detectors was done using an automated scanning track analysis system to obtain quantitative information on the pits produced in the CR-39. The system has a high quality microscope optical system (Nikon cfi series) operating at a magnification high enough to discriminate between tracks and background. The images obtained are then analyzed by the proprietary software. The software makes 15 characteristic measurements of each feature located in the image to provide reliable discrimination between etched tracks and background features present on or in the plastic detectors. These measurements include track length and diameter, optical density (average image contrast) and image symmetry.

2.5 SEM analysis of Pd/D co-deposited films

A series of external electric/magnetic field experiments were conducted in which the cathode substrate was gold foil. At the end of these experiments, SEM analysis of the Pd deposits on the Au foil was done using the Hitachi model S-4700 system.
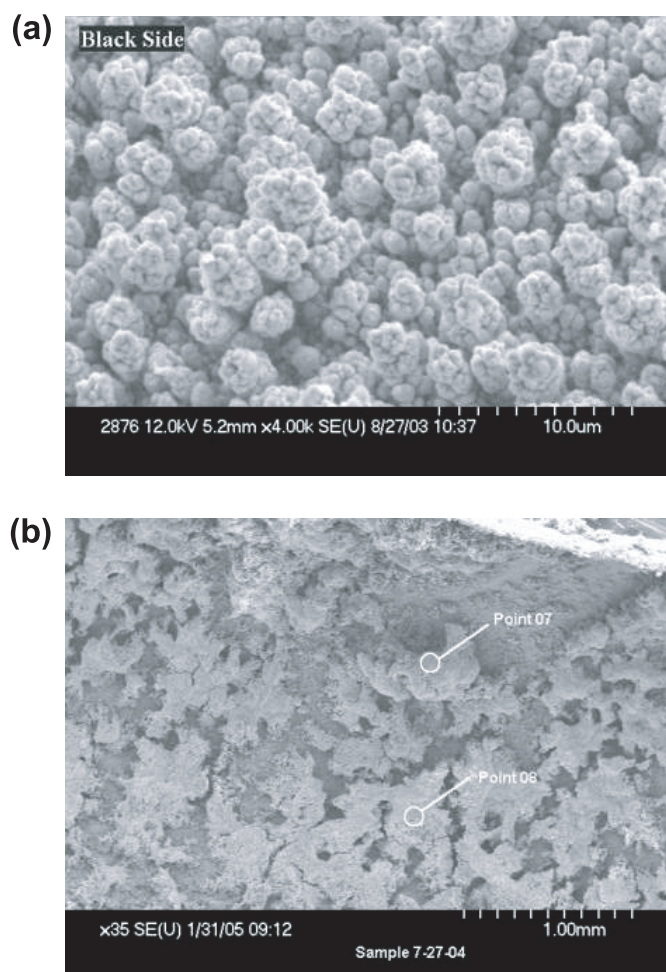
Fig. 2. SEM images of the Pd film deposited on Au foil obtained (a) in the absence of an external field and (b) after exposure to a magnetic field.

3 Results and discussion

3.1 Pd/D co-deposition on a Ni screen in the absence and presence of external electric or magnetic fields

In the Pd/D co-deposition experiment, the cathode and anode are immersed in a solution of palladium chloride and lithium chloride in deuterated water. Palladium is then electrochemically reduced onto the surface of the working electrode in the presence of evolving deuterium gas. Using the co-deposition technique, a high degree of deuterium loading (with an atomic ratio D/Pd > 1) is obtained within seconds [13–15]. In the absence of an external electric/magnetic field, SEM analysis shows that the Pd deposit has a uniform "cauliflower"-like structure, Figure 2a, and consists of aggregates of spherical micro-globules. In the presence of an external electric field [16], the following structural features were observed: branches (fractals), dendritic growths, craters, rods, wires, and folded thin films. Figure 2b shows the morphology of a Pd deposit that has been subjected to an external magnetic field. The Lorenz forces of the magnetic field have
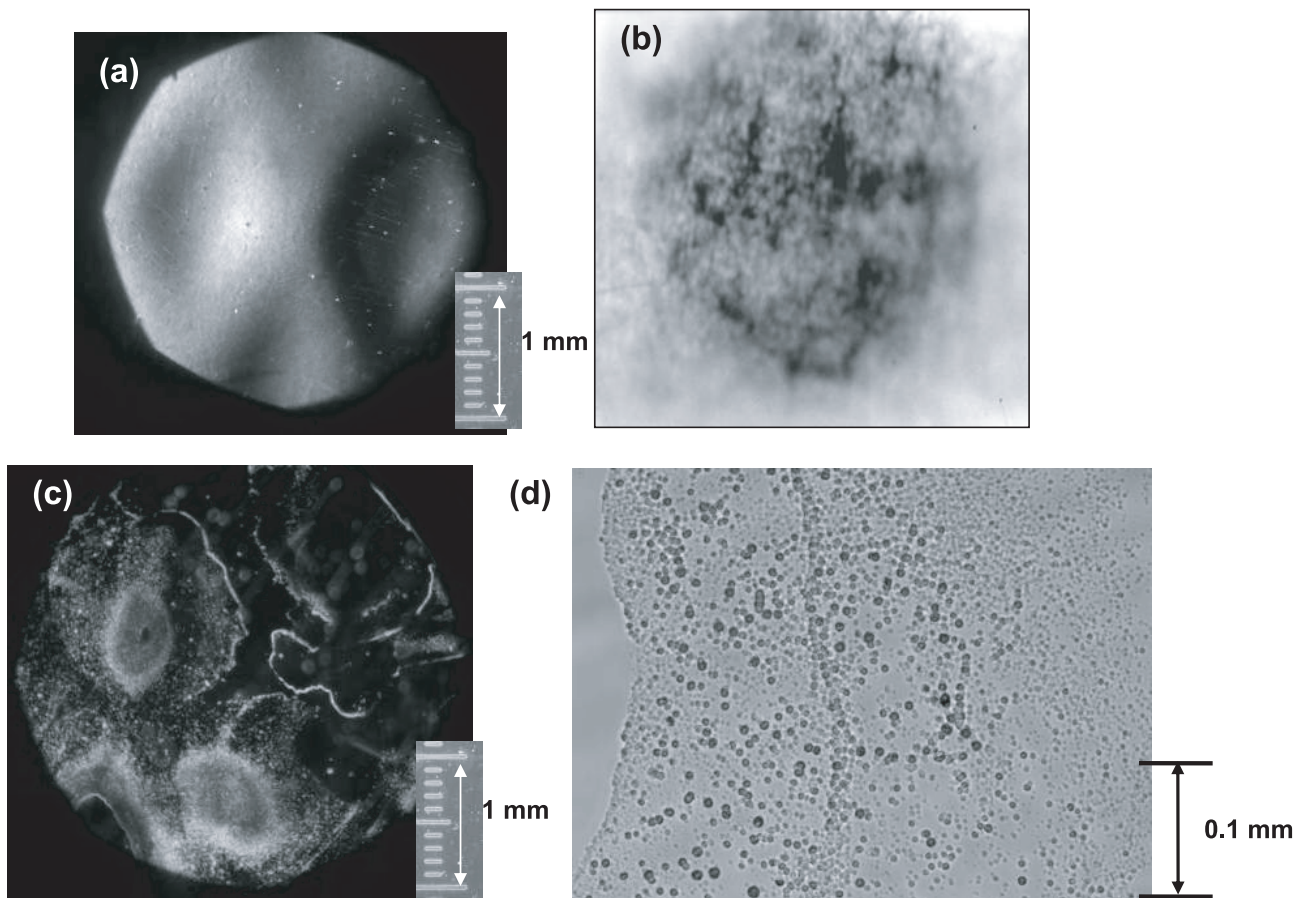
Fig. 3. (a) Microscopic image of the CR-39 detector that was in contact with the Pd film deposited on a Ni screen. This experiment was conducted in the absence of an external field. Magnification is 20X. (b) Fogging of photographic film after three days exposure to Pd deposited on a Ag disk cathode (thin Mylar separated the film and the cathode). Results of Pd/D co-deposited film that was subjected to an external magnetic field. Microscope images of the CR-39 detector that was in contact with the Pd film deposited on a Ni screen obtained using magnifications of (c) 20× and (d) 200×.

caused the Pd micro-globules to form the star-like features seen in Figure 2b. The development of these structural features in both the electric and magnetic field experiments require high energy expenditure. There are two energy transfer paths in operation during each experimental run – transfer from the external field and the electrochemical process, principally due to the absorption of deuterium [16]. These external field experiments were then conducted in the presence of CR-39 detectors.

In these experiments, the Pd/D co-deposition reaction was performed with the cathode in contact with the CR-39 detector, Figure 1. Because there is close proximity between the cathode and the detector, this geometry is most favorable for the detection of any particles that could potentially be emitted by the cathode. Experiments were first conducted using Ni screen as the substrate material onto which the Pd was plated out. Initial experiments were done in the absence of either an external electric or magnetic field. Figure 3a shows a 20× magnification of the CR-39 detector obtained after etching. Hollows are observed where the Pd had deposited inside the eyelet of the Ni screen. No pits were observed, even at higher magnifications. There have been previous reports of soft X-ray

emission by Pd/D substrates as measured using photographic film [17,18], HPGe γ-ray and Li doped Si X-ray detectors [19,20], and CaF$_2$ thermoluminescence dosimeters [9]. Figure 3b shows fogging of photographic film after a Pd/D co-deposition experiment conducted on the Ag disk of a piezoelectric crystal. The circular shape of the cathode can be seen and the emission of soft X-rays is not homogeneous over the surface of the cathode. It is therefore possible that the hollows observed in the CR-39 detector, Figure 3a, are the result of damage due to soft X-ray emission. Besides detection of energetic particles, there have been reports of using CR-39 to detect γ-rays [21–24] and soft X-rays [25]. It has been shown that CR-39 can be used in X-ray microscopy [25]. In the contact soft X-ray microscopy technique, the transmission X-ray image of a biological cell was recorded as latent damage on the CR-39 detector. After etching, the image of the cell was revealed as a relief on the polymer. To determine the effect of X-rays and γ-rays on CR-39, Cu screen was wrapped around two CR-39 detectors. One detector was placed inside an XRD and irradiated with X-rays while the other was exposed to a ^{137}Cs γ-ray source. After etching, the impression of the Cu screen was observed on the surface

of both CR-39 detectors. These results were similar to what was observed for the Pd/D co-deposition experiment in the absence of an external field and suggests that the damage summarized in Figure 3a is due to X-rays.

Significantly different results were obtained when either an external electric or magnetic field is applied across the Ni screen cathode. Figures 3c and 3d summarize the results obtained for the Pd/D co-deposition done on Ni screen in the presence of an external magnetic field (similar results are obtained when an external electric field is applied). In these experiments the external electric/magnetic field is applied after the Pd had been plated onto the electrode substrate. After etching, damage to the CR-39 detector is observed where Pd was in contact with the surface of the plastic. In the $20\times$ magnification, Figure 3c, the jagged outline of the Ni screen can be seen. Thousands of dots are observed in the figure. The density of dots is denser where the Pd deposit is the thickest, i.e., inside the eyelet of the Ni screen. Higher magnification of an area where the density of dots is lower shows that these dots are pits, Figure 3d. These results obtained using a Ni screen cathode indicate that the pits occur where the Pd is in contact with the CR-39 detector and only when either an external electric or magnetic field is applied. The overall size and shape of the pits are similar to nuclear tracks reported by Oriani and Fisher [10], Li [9], and Lipson et al. [11,12].

## 3.2 Nuclear tracks vs. chemical damage

Are the pits observed in Figures 3c and 3d tracks due to energetic particles or are they due to chemical damage? To determine this, the pits obtained from the Pd/D co-deposition experiment were compared with those obtained when CR-39 was exposed to an alpha particle source. Tracks created by an alpha source are conical in shape [26]. Figures 4a and 4b show images obtained for CR-39 exposed to an americium-241 source. Americium-241 decays to neptunium-237 by emitting alpha particles with the following energies and branching ratios: 5.378 MeV (1.4%), 5.433 MeV (13.6%), 5.476 MeV (84.4%), 5.503 MeV (0.21%), and 5.546 MeV (0.34%). Figure 4a is an image of the surface of the CR-39 while Figure 4b is an overlay of two images taken at two different focal lengths (one focal length is at the surface of the CR-39 detector and the other focal length is at the bottom of the pit). Figure 4a shows that the pits in the CR-39 detector caused by the ^{241}Am alpha particles are circular in shape and dark in color. When focusing deeper into the CR-39 detector, bright points of light are observed in the center of the pits, Figure 4b. These bright points are due to the bottom tip of the conical track. The pits also exhibit a high optical contrast. The optical contrast, shape, and bright spot in the center of the pit are used to differentiate between real particle tracks (which tend to be dark) from false events (which are often lighter in appearance and irregular in shape) [27,28]. Figures 5a–5d show images of pits in CR-39 obtained as the result of Pd/D co-deposition experiments. Dark, circular pits are observed that have
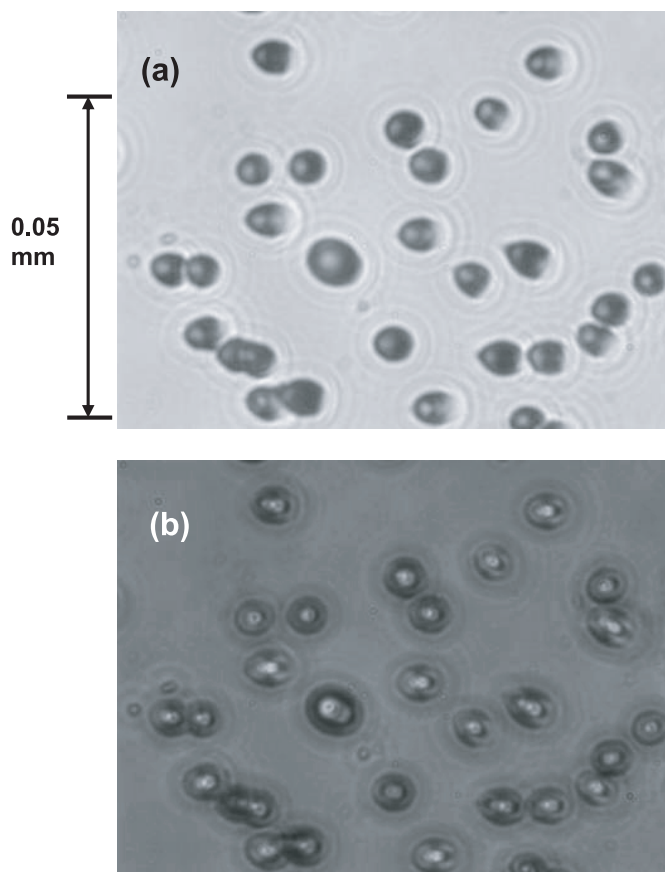
Fig. 4. Images of pits in CR-39 created by exposure to an ^{241}Am source, $1000\times$ magnification. (a) Focus on the surface of the CR-39. (b) Overlay of two images taken at two different focal lengths (surface and the bottom of the pits).

bright centers when focusing deeper into the plastic. In Figures 5a and 55b, both circular and elliptical (indicated by arrows in Fig. 5b) pits are observed. These features are consistent with those that are expected from authentic particle tracks. In Figure 5c, a mottled area in the plastic is observed (indicated by an arrow). The mottled area shows no contrast. The shapes are irregular. These features are consistent with chemical damage.

The results of incremental etching of a CR-39 detector are summarized in Figures S1 and S2 in the supplementary online materials. In this experiment, a corner of the CR-39 detector was exposed to an ^{241}Am source prior to conducting the Pd/D co-deposition reaction. At the end of the experiment, the CR-39 detector was etched for 9, 12, 16, and 20 h. Between etchings, images of the CR-39 detector were taken. In the case of the nuclear caused pits in the CR-39 detector resulting from the impingement of alpha particles from the ^{241}Am source, further etching of the CR-39 detector leads to an increase in the diameter of the pits, Figure S1 in the supplementary online materials. The pits remain dark and, when focusing deeper inside the CR-39, bright points of light are observed in the center of the pits The pits produced from the Pd/D co-deposition reaction, Figure S2 in the supplementary online materials, behave
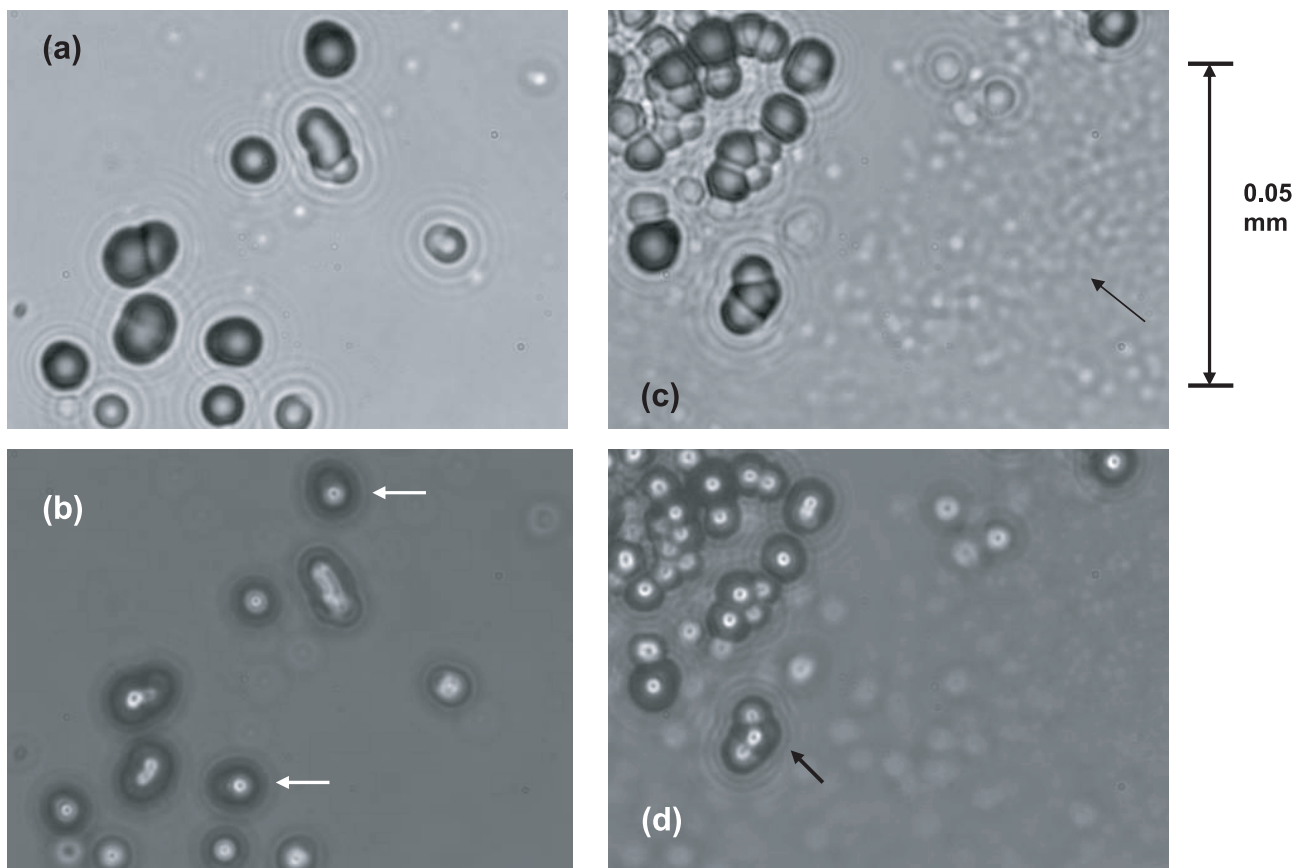
Fig. 5. Images of pits in CR-39 created as the result of a Pd/D co-deposition reaction. Ag wire, no external field experiment, $1000\times$ magnification. (a) and (c) Focus on the surface of the CR-39. (b) and (d) Overlay of two images taken at two different focal lengths (surface and the bottom of the pits). (b) Arrows indicate elliptical pits. (d) Arrow indicates a triple pit.

in the same manner. The incremental etching results support the conclusion that the pits observed in the CR-39 detector as a result of the Pd/D co-deposition process are nuclear in origin.

3.3 Control experiments

A series of experiments, summarized in Table 1, were conducted to verify that the formation of the pits is not due to contamination by radioactive nuclides or to the electrolysis process.

3.3.1 Contamination with radioactive nuclides

It has been suggested that the pits shown in Figures 3 and 5 are due to radioactive contaminants present in either the $PdCl_2$, LiCl, D_2O, or cathode substrates (Ni and Cu screens; Ag, Au, Pt, and Pd wires). To address this possibility, samples of the cathode substrates were wrapped around the CR-39 detectors and placed in a plastic cell containing either heavy or light water. Three weeks later (approximately the same amount of time required to complete each external field Pd/D co-deposition experiment),

no pits were observed that corresponded to the placement of the wires nor was the impression of the cathode substrates observed. Likewise no pits were observed when $PdCl_2$ powder was placed on the surface of a CR-39 detector or when a CR-39 detector was immersed in the $PdCl_2 - LiCl - D_2O$ electroplating solution. From these results it can be concluded that radioactive nuclides are not present in either the heavy or light water, $PdCl_2$, LiCl, or the cathode substrates.

3.3.2 Electrolysis

To verify that the pits observed in Figures 3 and 5 are not caused by the evolution of D_2 bubbles or the reducing conditions of the cathode, electrolysis experiments were conducted by wrapping either a Ni or Cu screen around a CR-39 detector. The Ni/Cu screen around CR-39 was then immersed in a solution of LiCl in D_2O. Electrolysis of D_2O, was achieved by applying a cathodic current of 50 mA. Vigorous gas evolution was observed on the cathode. After etching, no pits were observed where the Ni/Cu screen had been in contact with the CR-39 detector. There was also no impression of the Ni/Cu screen on the surface of the plastic. These results indicate that the pits are not due to the impingement of D_2 gas bubbles on the surface

Table 1. Summary of control experiments done in the absence of an external field.

Experiment[a]	Results of CR-39[b]
Pd, Ag, Au, and Pt wires in contact with CR-39 immersed in H_2O. No electrolysis.	No pits observed, no impression of the wires
$PdCl_2$ powder placed on top of CR-39. No electrolysis.	No pits observed
CR-39 detector placed in $PdCl_2 - LiCl - D_2O$ plating solution. No electrolysis.	No pits observed
Cu screen on CR-39 immersed in $LiCl - D_2O$ solution. Electrolysis $i = -50$ mA	No pits observed, no impression of the screen
Ni screen on Cr-39 immersed in $LiCl - D_2O$ solution. Electrolysis $i = -50$ mA	No pits observed, no impression of the screen

[a] Each experiment was conducted over a 2–3 week period.
[b] In this context, "No pits" is used to indicate that the number of pits observed was not in excess to what was commonly observed as a result of background emissions. Also what pits were observed were not directly associated with the placement of the cathode substrate in the cell.
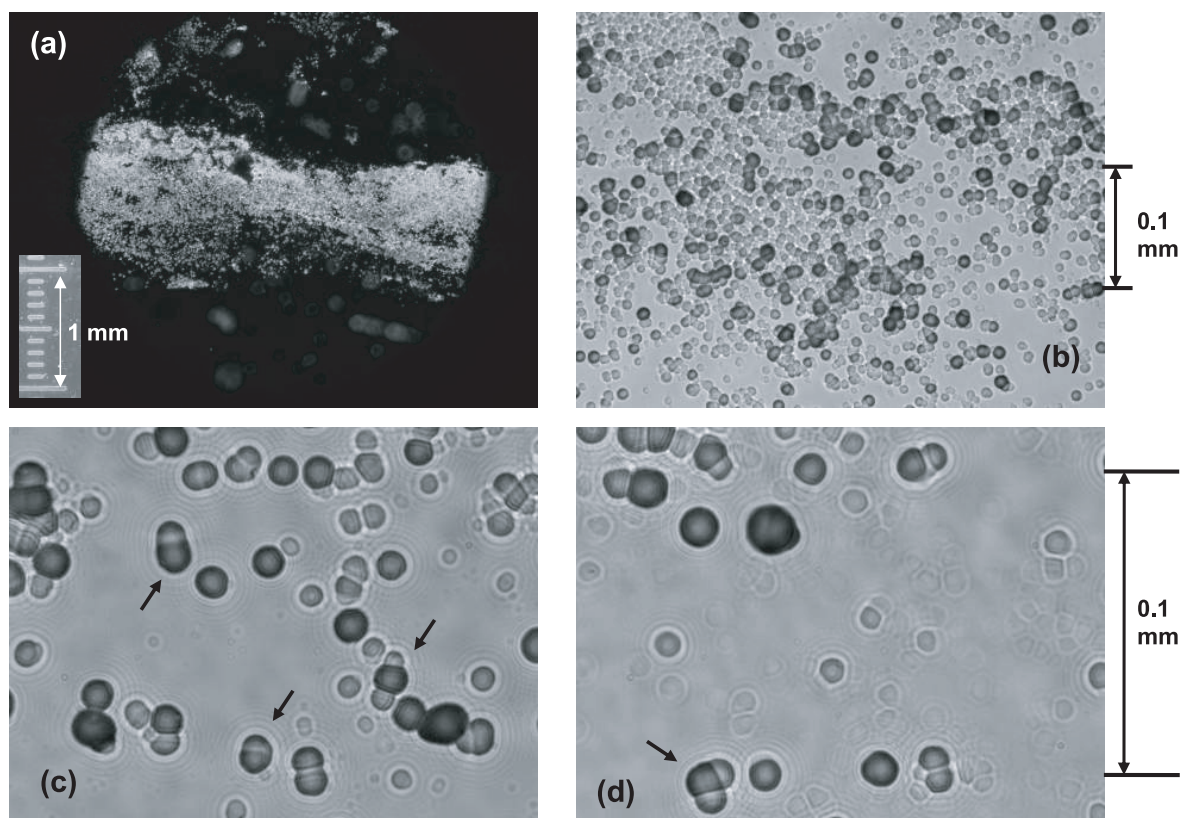
Fig. 6. Images of pits in CR-39 created as the result of a Pd/D co-deposition reaction. Ag wire, external magnetic field experiment. Magnifications: (a) 20×, (b) 200×, (c) 500×, and (d) 500×. Arrows in (c) and (d) indicate the presence of double and triple pits.

of the CR-39, reaction between D_2 and the CR-39, or from radioactive contaminants in either the Ni or Cu screens.

3.4 Results of additional experiments

Additional experiments, Table 2, were conducted to determine the components needed to generate pits in the CR-39 detectors.

3.4.1 Pd/D co-deposition on other cathode substrates

Experiments were conducted using higher Z cathodic substrates (Ag, Pt, and Au wires) for the Pd/D co-deposition. The results are summarized in Table 2 and Figure 6. In contrast with the Ni screen experiments, for higher Z cathodic substrates, an external field is not required to generate pits in the CR-39 detector. The difference could be attributed to either the electrode substrate or to the

Table 2. Summary of experiments used to determine the components necessary to generate pits in the CR-39 detector.

Experiment[a]	Field	Results of CR-39[b]
Ni screen in contact with CR-39, electrolysis in $PdCl_2 - LiCl - D_2O$ solution	No field	No pits observed. See hollows in CR-39 where Pd plated out in the eyelets of the Ni screen
Ni screen in contact with CR-39, electrolysis in $PdCl_2 - LiCl - D_2O$ solution	Either Electric or Magnetic	High density of pits observed where Pd was in contact with the Ni screen
3 wires (Au, Ag, Pt) in series in contact with CR-39, electrolysis in $PdCl_2 - LiCl - D_2O$ solution	Either Electric or Magnetic	High density of pits observed where Pd was in contact with wires
3 Ag wires in parallel in contact with CR-39, electrolysis in $PdCl_2 - LiCl - D_2O$ solution, run 1 wire for 1 h, second for 2 h, third for 4 h	Electric	Bursts of pits only observed for the wire that ran for 1 h
3 Au wires in parallel in contact with CR-39, electrolysis in $PdCl_2 - LiCl - D_2O$ solution, run 1 wire for 24 h, second for 48 h, third for 72 h	Electric	Pits observed where Pd was in contact with wires. Density less than observed for longer running experiments
Pd wire in contact with CR-39, electrolysis in $LiCl - D_2O$ solution	No field; Either Electric or Magnetic	See hollow where Pd wire was in contact with CR-39 detector. See bursts of pits. Density of pits far less than observed for Pd/D co-deposition
Au, Pt, or Ag wire in contact with CR-39, electrolysis in $PdCl_2 - LiCl - D_2O$ solution	No field, Either Electric or Magnetic	High density of pits observed where Pd was in contact with wires
Ag wire in contact with CR-39, electrolysis in $PdCl_2 - LiCl - H_2O$ solution	Either Electric or Magnetic	See hollow where Pd that was deposited on the wire was in contact with CR-39 detector. See bursts of pits. Density of pits far less than observed for Pd/D co-deposition
Ag wire in contact with CR-39, electrolysis in $PdCl_2 - KCl - D_2O$ solution	Either Electric or Magnetic	High density of pits observed where Pd was in contact with wire
Ag wire in contact with CR-39, electrolysis in $CuCl_2 - LiCl - D_2O$ solution	No field, Either Electric or Magnetic	Clear, up-raised area observed where Cu deposit was in contact with CR-39; no pits observed.

[a] Except for the Pd wire experiments and three wires in parallel, each experiment was conducted over a 2–3 week period. Pd wire experiments conducted over a 5 week period.

[b] In this context, 'No pits' is used to indicate that the number of pits observed was not in excess to what was commonly observed as a result of background emissions. Also what pits were observed were not directly associated with the placement of the cathode substrate in the cell.

current density (the individual wires will exhibit a higher current density than the screen). Regardless of the high Z cathode substrate used for the Pd/D co-deposition, cloudy areas were observed where the Pd-coated wires were in contact with the CR-39, Figure 6a. Higher magnification shows that within these cloudy areas there are copious numbers of pits, Figure 6b. The density of pits decreases the further away one gets from the Pd film deposited on the wire. In the areas where the density of pits is less, Figures 6c and 6d, it can be see that there are both large and small pits as well as double and triple pits (indicated by arrows). Double and triple pits result from reactions that emit two or three particles of similar mass and energy [7,25]. A triple pit is also observed in Figures 5c and 5d (indicated by an arrow in Fig. 5d). Figure S3 in the supplementary online materials shows a

45× digital magnification of the triple pit shown in Figure 5d. As indicated vide supra, Figure 5d is an overlay of two images taken at two different focal lengths. One focal length is at the surface of the CR-39 detector, the other focal length is at the bottom of the pit. When the triple pit is magnified, Figure S3 in the supplementary online materials, it appears that the two side pits are splitting away from the central pit.

Two sets of temporal experiments were conducted to determine when the evolution of pits occurred. In these experiments, three wires of the same type were in contact with the CR-39. The wires were in parallel, meaning a wire could be disconnected without affecting the other wires. Results are summarized in Table 2. After the Pd had been plated out, the current was increased. In the Ag wire experiment. One wire underwent electrolysis for

1 h, another for 2 h, and the third for 4 h. Pits were observed on the CR-39 for only the 1 h exposure [29]. In the Au wire experiment, the current over all three wires was maintained at 20 mA. One wire ran for 24 h, another for 48 h, and the third for 72 h. In this experiment, the density of pits was less than was observed in the longer term experiments. Both the Ag and Au temporal experiments suggest that the emission of the high energy particles occurs in bursts. This is consistent with earlier Pd/D co-deposition results the evolution of hot spots as imaged using an infrared camera [30] and the sporadic production of tritium [31] and heat [32].

3.4.2 LiCl vs. KCl

Pd/D co-deposition experiments were conducted in D_2O where the background electrolyte LiCl was replaced with KCl. As the results summarized in Table 2 indicate, no difference was observed when KCl was substituted for LiCl.

3.4.3 Heavy vs. light water

Results of light water experiments are summarized in Table 2 and Figures S4a and S4b in the supplementary online materials. Visual inspection of the post-etch CR-39 detector used in a light water, external electric field experiment showed a furrow that corresponded to the placement of the Ag wire that was used as the substrate for the Pd/D co-deposition. As discussed vide supra, the furrow could be indicative of damage due to the emission of soft X-rays. Sparse patches of cloudy areas are observed along this furrow. Figure S4a is a $20\times$ magnification of one such patch. Higher magnification, Figure S4b in the supplementary online materials, shows the presence of pits. These results are consistent with the reports of energetic particles [12] and X-ray emission [19] for light water electrolysis experiments using thin Pd foils. Compared to results obtained for heavy water, the density of pits is far less in the light water experiments.

3.4.4 Pd/D wire vs. Pd/D co-deposition

Experiments were conducted using a Pd wire in place of the Pd/D co-deposited film. Results are summarized in Figures S4c and S4d in the supplementary online materials. A furrow in the CR-39 detector was observed where the Pd wire was in contact with the detector. Scattered cloudy areas were observed along this furrow. The furrow is believed to be damage caused by the emission of soft X-rays from the Pd wire. Figures S4c and S4d show $20\times$ and $200\times$ magnifications of one cloudy area which show the presence of pits. The density of pits is far less than what was observed for the Pd/D co-deposition experiments. Pits only occur in the CR-39 detector that is in contact with "active" areas of the Pd wire. It has been well documented that, in the case of bulk Pd, generation of heat, tritium, and helium does not occur homogeneously throughout the Pd [33]. Some areas in the bulk Pd show greater activity than others. Another suggestion has been made that the pits are caused by the tips of the Pd dendrites formed during the Pd/D co-deposition either piercing the surface of the CR-39 or producing hydroxide ions that etch pits into the CR-39. Since pits are observed using a Pd wire which has no dendritic structure to it, neither of these suggested mechanisms of pit formation (piercing or localized etching) is valid.

3.4.5 Cu electrodeposition experiments

Additional experiments were conducted using $CuCl_2$ in place of the $PdCl_2$. The electrochemical reactions for both the $CuCl_2$ and $PdCl_2$ systems are essentially the same. Metal plates out in the presence of evolving D_2 gases at the cathode and O_2 and Cl_2 evolution will occur at the anode. The metal deposits formed for both Pd and Cu are similar – dendritic with high surface area. The only significant difference is that Pd absorbs deuterium and Cu does not. The CR-39 detector results are summarized in Table 2. After etching the CR-39 detector that was in contact with the Ag/Cu cathode, a clear, upraised area was observed where the Cu deposit had been in contact with the CR-39, Figure S5a in the supplementary online materials. No pits were observed on or near this upraised area. However some mottled areas were observed. Higher magnification of these areas, Figure S5b in the supplementary online materials, shows the presence of shallow, irregularly shaped features that are consistent with chemical damage. No pits on the CR-39 detector were observed upon application of an external electric/magnetic field. The Cu electroplating results further indicate that the pits observed in these experiments are not due to the dendrites piercing into the CR-39 or to localized production of hydroxide ions that etch into the CR-39. These results also indicate that dendrite enhanced fusion is not occurring. According to the dendrite enhanced fusion model [34], the dendrite tips exhibit a high surface potential where local dielectric breakdown occurs to form D^+ ions which are accelerated along field lines into adsorbed deuterons to create fusion products. Such a mechanism does not require a hydrogen absorbing material such as Pd.

3.5 Quantitative analysis of the CR-39 pits

Figure 7 shows the results of quantitative analysis of pits in CR-39 obtained using the automated track analysis system. Figures 7a and 7b show the size distribution of pits and a plot of minor axis vs. major axis measured for a CR-39 detector that had been exposed to depleted uranium. ^{238}U emits a 4.27 MeV alpha. The results shown in Figure 7a show that the pits can be separated into three size distributions: 0.9–1.9 μm, 1.9–4.0 μm, and 4.1–16 μm. Figure 7b is a plot of minor axis vs. major axis. This plot is a measure of the ellipicity of the pits. An alpha particle that hits normal to the plane of the CR-39 will leave a circular pit whose minor axis approximately equals the
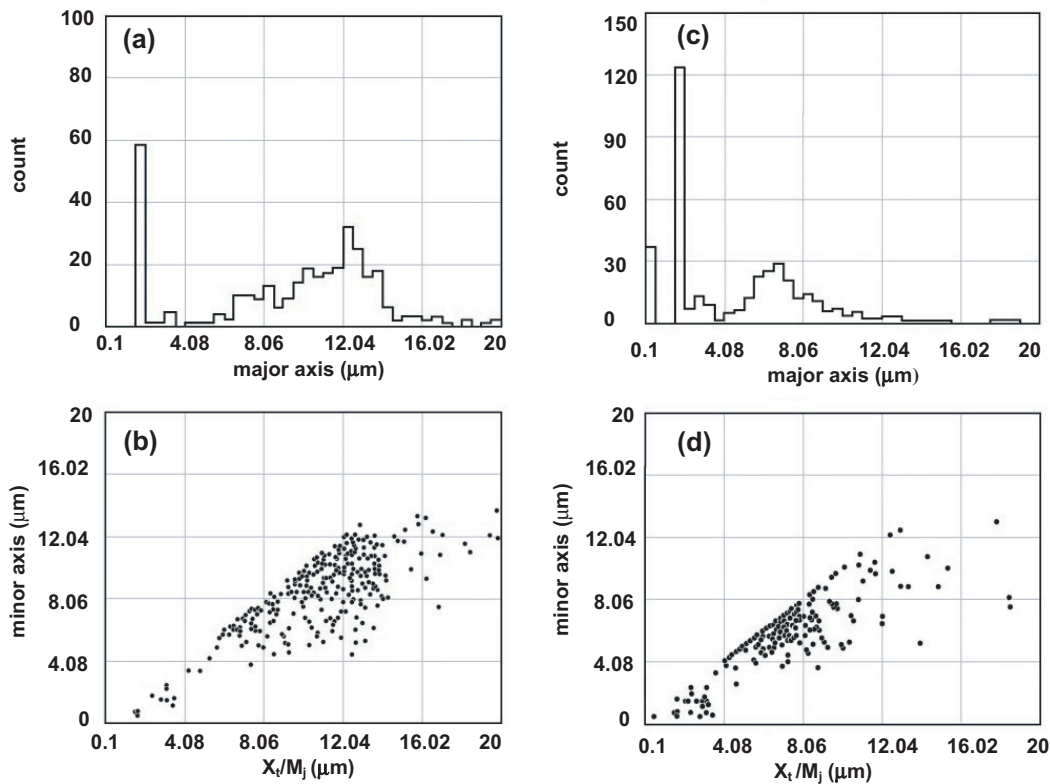
Fig. 7. Quantitative analysis of pits obtained by exposing CR-39 to depleted uranium ($N = 333$ pits): (a) size distribution, (b) minor axis vs. major axis. Quantitative analysis of pits obtained for CR-39 subjected to a Pd/D co-deposition experiment conducted on a Au wire in the presence of an external magnetic field ($N = 388$ pits): (c) size distribution, (d) minor axis vs. major axis. Note: X_t/M_j, is the major axis and, depending upon the angle of incidence, may include the tail.

major axis. Conversely, an alpha particle that does not hit normal to the plane of the CR-39 will leave an elliptical pit whose major axis will be larger than the minor axis. Figure 7b shows that both circular and elliptical pits are formed in CR-39 upon exposure to depleted uranium.

Similar results are obtained from the quantitative analysis of a CR-39 detector that has been subjected to a Pd/D co-deposition experiment. Figure 7c shows that the pits can be separated into three size distributions: 0.1–0.5 μm, 0.9–4.0 μm, and 4.1–12 μm. The minor axis vs. major axis plot, Figure 7d, shows that both circular and elliptical pits are observed. The large and small pits, indicated in Figure 7c, could be caused by different classes of particles, e.g. protons and alphas as was shown by Lipson et al. [11,12], or they could be different energies for the same class of particles. Additional work, using spacer materials, needs to be done to determine whether or not different classes of particles are present as well as their energies.

4 Conclusions

The formation of pits in CR-39 etch track detectors have been observed to occur during Pd/D co-deposition experiments. The experiments are reproducible. The pits are dark and circular in shape and have bright centers when focusing deeper in the plastic. Quantitative analysis shows that there are three populations of pits (0.1–0.5 μm, 0.9–4.0 μm, and 4.1–12 μm) and that the pits can be either perfectly circular or elliptical in shape. These features are consistent with those observed for nuclear generated pits. In this communication, it has been shown that the pits formed during Pd/D co-deposition are not due to radionuclide contamination of the cell components nor are they caused by impingement of gas bubbles on the surface of the CR-39. Since electrochemical plating of $CuCl_2$ did not result in pits, production of pits in a Pd/D co-deposition experiment cannot be attributed to chemical attack of the surface of CR-39 by either D_2, O_2, or Cl_2 present in the electrolyte. Additional experiments showed that LiCl is not essential for the production of pits and that the density of pits significantly decreases when H_2O is substituted for D_2O or when a Pd wire is substituted for Pd/D co-deposition.

References

1. T. Yamauchi, Radiat. Meas. **36**, 73 (2003)
2. J.R. Bhakta, G.D. Hardcastle, J.C.H. Miles, Radiat. Meas. **30**, 29 (1999)
3. D. Nikezic, K.N. Yu, Materials Sci. Eng. R **46**, 51 (2004)
4. R. Ilić, J. Skvarć, A.N. Golovchenko, Radiat. Meas. **36**, 83 (2003)
5. V.S. Belyaev, A.P. Matafonov, V.I. Vinogradov, V.P. Krainov, V.S. Lisitsa, A.S. Roussetski, G.N. Ignatyev, V.P. Andrianov, Phys. Rev. E **72**, 26406 (2005)
6. F.H. Séguin, J.A. Frenje, C.K. Li, D.G. Hicks, S. Kurebayashi, J.R. Rygg, B.-E. Schwartz, R.D. Petrasso, S. Roberts, J.M. Soures, D.D. Meyerhofer, T.C. Sangster, J.P. Knauer, C. Sorce, V. Yu. Glebov, C. Stoeckl, T.W. Phillips, R.J. Leeper, K. Fletcher, S. Padalino, Rev. Sci. Instrum. **74**, 975 (2003)
7. J.K. Pálfalvi, Y. Akatov, L. Sajó-Bohus, J. Szabó, I. Eördögh, Cosmic Particle Induced Reaction Detection with SSNTD Stacks Exposed On-Board of the International Space Station, in *10th International Conference on Nuclear Reaction Mechanisms, Varenna, Villa Monastero-Italy, June 9–13, 2003*
8. D.L. Henshaw, Phys. Technol. **13**, 266 (1982)
9. X.Z. Li, The Precursor of Cold Fusion Phenomenon in Deuterium/Solid Systems, in *Anomalous Nuclear Effects in Deuterium/Solid Systems, AIP Conference Proceedings* (Brigham Young Univ., Provo, UT: American Institute of Physics, New York, 1990), 228
10. R.A. Oriani, J.C. Fisher, Jpn J. Appl. Phys. **41**, 6180 (2002)
11. A.G. Lipson, A.S. Roussetski, G.H. Miley, E.I. Saunin, Phenomenon of an Energetic Charged Particle Emission From Hydrogen/Deuterium Loaded Metals, in *Tenth International Conference on Cold Fusion* (Cambridge, MA, 2003), `LENR-CANR.org`
12. A.G. Lipson, A.S. Roussetski, G.H. Miley, C.H. Castano, In-Situ Charged Particles And X-Ray Detection In Pd Thin Film-Cathodes During Electrolysis In Li_2SO_4/H_2O, in *The 9th International Conference on Cold Fusion, Condensed Matter Nuclear Science, Beijing, China* (Tsinghua University, Tsinghua Univ. Press, 2002)
13. S. Szpak, P.A. Mosier-Boss, S.R. Scharber, J.J. Smith, J. Electroanal. Chem. **337**, 147 (1992)
14. S. Szpak, P.A. Mosier-Boss, J.J. Smith, J. Electroanal. Chem. **379**, 121 (1994)
15. S. Szpak, P.A. Mosier-Boss, S.R. Scharber, J.J. Smith, J. Electroanal. Chem. **380**, 1 (1995)
16. S. Szpak, P.A. Mosier-Boss, C. Young, F.E. Gordon, J. Electroanal. Chem. **580**, 284 (2005)
17. M. Miles, B.F. Bush, J.J. Lagowski, Fusion Technol. **25**, 478 (1994)
18. S. Szpak, P.A. Mosier-Boss, J.J. Smith, J. Electroanal. Chem. **302**, 255 (1990)
19. S. Szpak, P.A. Mosier-Boss, J.J. Smith, Phys. Lett. A **210**, 382 (1995)
20. V. Violante, P. Tripodi, D. Di Gioacchino, R. Borelli, L. Bettinali, E. Santoro, A. Rosada, F. Sarto, A. Pizzuto, M.C.H. McKubre, F. Tanzella, X-ray emission during electrolysis of light water on palladium and nickel thin films, in *The 9th International Conference on Cold Fusion, Condensed Matter Nuclear Science, Tsinghua Univ., Beijing* (Tsinghua Univ. Press, China, 2002)
21. S. Singh, S. Prasher, Nucl. Instrum. Meth. Phys. Rev. B **222**, 518 (2004)
22. AH. Ranjbar, S.A. Durrani, K. Randle, Radiat. Meas. **28**, 831 (1997)
23. A.F. Saad, S.T. Atwa, R. Yokota, M. Fujii, Radiat. Meas. **40**, 780 (2005)
24. S.E. San, J. Radiol. Prot. **25**, 93 (2005)
25. K. Amemiya, H. Takahashi, M. Nakazawa, H. Shimizu, T. Majima, Y. Nakagawa, N. Yasuda, M. Yamamoto, T. Kageji, M. Nakaichi, T. Hasegawa, T. Kobayashi, Y. Sakurai, K. Ogura, Nucl. Instrum. Meth. Phys. Rev. B **187**, 361 (2002)
26. A.M. Abdel-Moneim, A. Abdel-Naby, Radiat. Meas. **37**, 15 (2003)
27. S.H. Séguin, J.A. Frenje, C.K. Li, D.G. Hicks, S. Kurebayashi, J.R. Rygg, B.-E. Schwartz, R.D. Petrasso, S. Roberts, J.M. Soures, D.D. Meyerhofer, T.C. Sangster, J.P. Knauer, C. Sorce, V. Yu Clebov, C. Stoeckl, T.W. Phillips, R.J. Leeper, K. Fletcher, S. Padalino, Rev. Sci. Instrum. **74**, 975 (2003)
28. J.P.Y. Ho, C.W.Y. Yip, D. Nikezie, K.N. Yu, Radiat. Meas. **36**, 155 (2003)
29. S. Szpak, P.A. Mosier-Boss, F.E. Gordon, Naturwissenschaften **94**, 511 (2007)
30. P.A. Mosier-Boss, S. Szpak, Nuovo Cimento Soc. Ital. Fis. A **112**, 577 (1999)
31. S. Szpak, P.A. Mosier-Boss, R.D. Boss, J.J. Smith, Fusion Technol. **33**, 38 (1998)
32. S. Szpak, P.A. Mosier-Boss, M.H. Miles, M. Fleischmann, Thermochim. Acta **410**, 101 (2004)
33. E. Storms, Some Thoughts on the Nature of the Nuclear-Active Regions in Palladium, in *the Sixth International Conference on Cold Fusion, Progress in New Hydrogen Energy* (Tokyo Institute of Technology, Tokyo, Japan, 1996)
34. J.O'M. Bockris, G.H. Lin, R.C. Kainthla, N.J.C. Packham, O. Velev, Does Tritium Form at Electrodes by Nuclear Reactions. in *the First Annual Conference on Cold Fusion* (University of Utah Research Park, Salt Lake City, Utah, 1990)